Dielectric spectra and electrical conduction in Fe-doped $SrTiO_3$

Chen Ang* and Zhi Yu*
Institut für Physik, Universität Augsburg, D-86135 Augsburg, Germany

Zhi Jing
Department of Ceramics and Glass Engineering, University of Aveiro, 3810 Aveiro, Portugal

P. Lunkenheimer and A. Loidl
Institut für Physik, Universität Augsburg, D-86135 Augsburg, Germany
(Received 1 April 1999; revised manuscript received 30 June 1999)

The transport and dielectric properties of $Sr_{0.97}(Ti_{1-x}Fe_x)O_{3-\delta}$ solid solutions have been investigated at temperatures $1.5\ K \leqslant T \leqslant 300\ K$ and frequencies $20\ Hz \leqslant \nu \leqslant 1\ MHz$. Depending on x, suppression of the quantum-paraelectric background, dielectric anomalies associated with relaxational processes, variable-range-hopping conduction, and a sublinear power-law increase in the ac conductivity were observed. The results of the present work are the following: (i) For low concentration Fe doping, the suppression of the paraelectric state is smaller than for Bi and La doping; the higher stability of the quantum paraelectric state is due to the fact that, in contrast to Bi and La, Fe substitutes for Ti sites. (ii) The observed variable-range-hopping (VRH) conduction indicates that Fe doping leads to the occurrence of local states in the highly disordered $SrTiO_3$ lattice; this behavior coexists with the stable quantum paraelectric state. (iii) A dielectric relaxation process from 50 to 200 K is observed that is related to some defects; it is evidenced that the dielectric relaxation has no direct relation with the VRH mechanism, however, it is very possibly related to a polaron mechanism.

I. INTRODUCTION

$SrTiO_3$-based perovskite oxides are technically important materials and also of interest from a more fundamental point of view. The continuous increase of the permittivity with decreasing temperature and the leveling off of the permittivity at very low temperatures is explained by the softening of phonon modes and quantum fluctuation effects, respectively.[1,2] At low temperatures, the paraelectric state is stabilized by the zero-point energy. There are various reports on the effects of impurity doping on the properties of this interesting system.[3–6] For substitutions of the Sr site the suppression of the quantum paraelectric state was reported.[3–9] Bi doping leads to the occurrence of several polarization modes and final transition to ferroelectric relaxor behavior.[6–8] La doping strongly suppresses the paraelectric state, however, no intrinsic polarization modes occur, except for polarization effects related to oxygen vacancies.[9] $SrTiO_3$ doped with Fe combines the required stability and interesting transport properties at relatively high temperatures. In this case, Fe^{3+} substitutes for Ti^{4+}. The material has been considered for application as electrochemical electrodes and resistive oxygen sensors.[10–12] For these applications, special attention was paid to the electrical transport properties at high temperatures. In a previous paper,[13] some of the present authors reported the observation of dielectric relaxation processes and a variable-range-hopping (VRH) conduction in the temperature range 50–300 K for $SrTiO_3$ doped with Fe. In the present paper, we extend the temperature range down to 1.5 K, to clarify the possible mechanisms of the dielectric relaxation process and to study the VRH conduction in detail. In addition, we briefly comment on differences in dielectric relaxation when substituting on the Ti site or on the Sr site in $SrTiO_3$.

II. EXPERIMENTAL PROCEDURE

Ceramic samples with composition $Sr_{0.97}(Ti_{1-x}Fe_x)O_{3-\delta}$ ($x=0.02$, 0.05, 0.1, and 0.2) were prepared by solid-state reaction. A 3% atomic Sr-site deficiency was introduced to enhance the chemical stability.[14] In order to check for the effect of the cooling rate after sintering, two samples with $x=0.2$ were prepared with slow cooling (cooled in furnace) and quenched process (quenched from sintering temperatures), respectively.

Dielectric and conductivity measurements were made using the HP 4284A LCR meter and Solartron 1260 Impedance Gain-Phase Analyzer, and a Keithley-617 Programmable Electrometer. For the measurements the samples were coated with silver and/or In-Ga electrodes. The x-ray-diffraction (XRD) results indicated that all samples were single phase and exhibited the cubic perovskite structure.[13]

III. RESULTS AND DISCUSSION

A. Investigation of the quantum-paraelectric background for $0.02 \leqslant x \leqslant 0.1$

The temperature dependence of the real (ϵ') and imaginary (ϵ'') part of the complex dielectric permittivity for Fe-doped $SrTiO_3$ ($x=0.02$) is shown in Fig. 1 for various frequencies. With decreasing temperature, ϵ' increases continuously and saturates at low temperatures, revealing the characteristic quantum paraelectric behavior. The leveling off of the ϵ' at the low temperatures, similar to that of the pure $SrTiO_3$, is more clearly seen in the plot with the logarithm scale of the temperature axis, as shown in Fig. 2, for $x=0.02$, 0.05, and 0.1 at 100 Hz. From Fig. 1, it can be seen that small relaxational processes are superimposed on the background of the pure $SrTiO_3$-like in $\epsilon'(T)$ from 50 to 200 K, which can be more easily observed in the $\epsilon''(T)$.

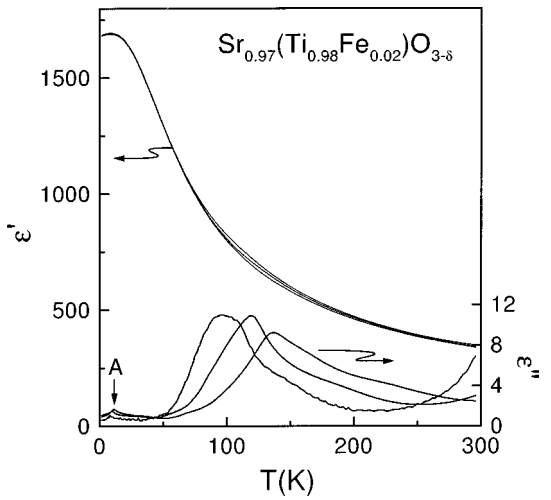

FIG. 1. Temperature dependence of ϵ' and ϵ'' for the sample $Sr_{0.97}(Ti_{1-x}Fe_x)O_{3-\delta}$ with $x=0.02$ at frequencies 0.1, 1, and 10 kHz (from left to right for ϵ', from top to bottom for ϵ'', respectively). ''*A*'' denotes the low-temperature relaxation.

In Fig. 1, for $x=0.02$, an additional frequency-dispersive loss peak (marked as ''*A*'') is observed around 10 K. A similar relaxation process has been found in nominally pure $SrTiO_3$ and Bi-doped $SrTiO_3$, and is discussed in detail in Ref. 8.

It is known that the paraelectric state of pure $SrTiO_3$ can be described by the Barrett relation,[15] which is based on the mean-field theory taking quantum fluctuations into account:

$$\epsilon' = C/[(T_1/2)\coth(T_1/2T) - T_0]. \quad (1)$$

Here C is the Curie-Weiss constant, T_1 represents the tunneling integral, and T_0 is the transition temperature where the lattice instability would occur in the absence of quantum fluctuations.

Fits of the experimental data to the Barrett relation, Eq. (1), are shown in Fig. 2. The fit parameters for the different concentrations are also indicated in Fig. 2. The series of parameters C and T_1 agree well with those reported for a pure

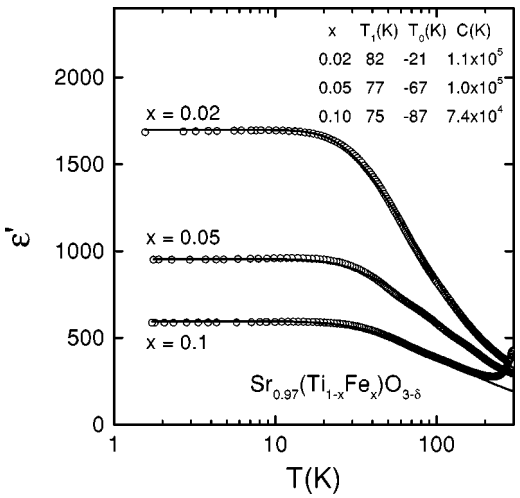

FIG. 2. Temperature dependence of ϵ' for the samples with $x=0.02$, 0.05, and 0.1 at 100 Hz. Solid lines: fits to Barrett relation, Eq. (1); the fitting parameters are noted in the figure.

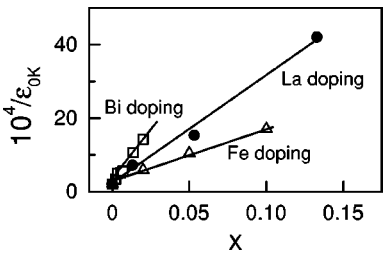

FIG. 3. Concentration dependence of inverse $\epsilon'(0\ \mathrm{K})$ for $Sr_{0.97}(Ti_{1-x}Fe_x)O_3$, with $x=0.02$, 0.05, and 0.1. For comparison, the data of $(Sr_{1-1.5x}Bi_x)TiO_3$ and $(Sr_{1-1.5x}La_x)TiO_3$ are also shown.

single crystal $SrTiO_3$ by Müller and Burkard ($T_1=84$ K, $C=0.9\times10^5$ K, and $T_0=38$ K).[1] However, T_0 is strongly reduced for the doped samples, and is negative. The positive value of $(T_1\text{-}2T_0)$ is a signature of the quantum paraelectric behavior; the higher the value of $(T_1\text{-}2T_0)$, the more stable the paraelectric state.[1,15] In this work, with increasing Fe doping concentration, the values of $(T_1\text{-}2T_0)$ increase, implying that Fe doping drives the system away from the ferroelectric instability.

As seen in Fig. 2, the low-temperature dielectric constant is strongly reduced with increasing Fe concentration x. That is, Fe doping strongly suppresses the polarization at low temperatures. In Fig. 3, inverse $\epsilon'(T\rightarrow0\ \mathrm{K})$ (denoted as $[\epsilon'(0\mathrm{K})]^{-1}$) is plotted versus x. For comparison, the data of Bi and La-doped $SrTiO_3$ are included in Fig. 3. It is found, that in the three systems investigated $[\epsilon'(0\mathrm{K})]^{-1}$ increases linearly on concentration. A similar behavior was also reported for Li-doped $KTaO_3$ by Höchli *et al.*[16] At present, the microscopic nature of this linear relation is unclear. A closer inspection of Fig. 3 reveals that the slope of $[\epsilon'(0\mathrm{K})]^{-1}$ vs x for Bi doping is about two times larger than that for La doping, and four times larger than for Fe-doped samples. Bi^{3+} substitutes for Sr^{2+}, which is a highly polarizable ion tending to induce polar clusters. The observation of relaxor behavior in Bi-doped $SrTiO_3$ fits well to this frame,[6,8] and obviously these polar clusters must effectively suppress quantum fluctuations. La^{3+} which also substitutes at the Sr site, but is much less polarizable, has a much smaller influence on the quantum fluctuations. Different from Bi and La doping, Fe substitutes on the Ti site, and has the minimum slope; this means that the Fe substitution at Ti sites does not cause polar clusters, and it has a smaller effect than those of the Bi and La doping.

B. dc conductivity

The temperature dependence of the dc conductivity σ_{dc} for $x=0.1$ and $x=0.2$ is shown in Fig. 4. The results indicate that $\sigma_{\mathrm{dc}}(T)$ cannot be fitted assuming a thermally activated conduction mechanism, which is commonly used to characterize band conduction. In this case, σ_{dc} should follow $\sigma_{\mathrm{dc}}=\sigma_0\exp[-E_{\mathrm{cond}}/k_BT]$, where σ_0 is the pre-exponential term, and E_{cond} is the activation energy for conduction. The Arrhenius plot shown in the inset of Fig. 4 does not lead to straight lines over significant temperature ranges. However, a satisfactory result can be obtained assuming a VRH mechanism[17]

$$\sigma_{dc}=\sigma_0\exp(-T_0/T)^{1/4}, \quad (2)$$

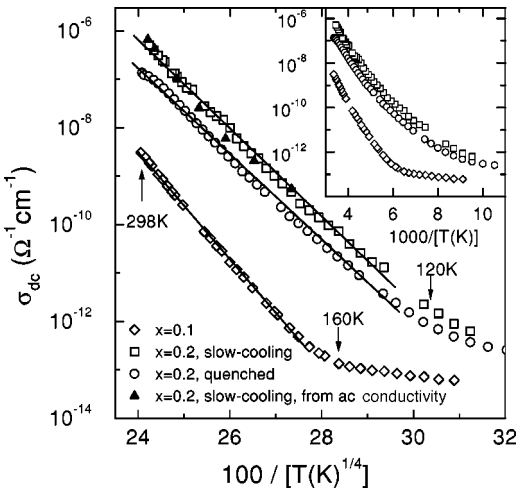

FIG. 4. Temperature dependence of the dc conductivity for $x=0.1$ and 0.2 (quenched and slow cooled during preparation). In the main frame a representation was chosen that leads to a straight line for VRH. The solid lines are fits to the VRH prediction, Eq. (2). The triangles are the values of σ'_{dc} as determined from the low-frequency plateau of $\sigma'(\nu)$ for the slow-cooling sample with $x=0.2$ (see Fig. 6). The inset shows the data in Arrhenius representation.

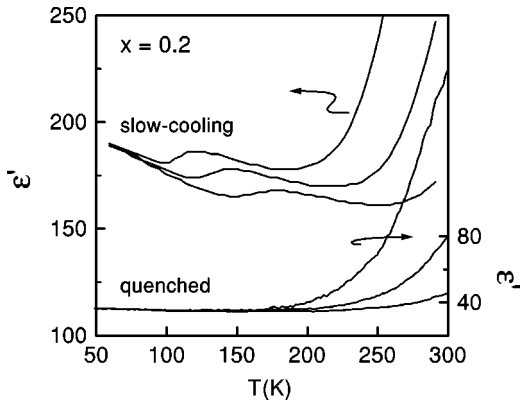

FIG. 5. Temperature dependence of ϵ' and ϵ'' for the two $x=0.2$ samples (slow cooled and quenched during preparation). The frequencies are (from top to bottom): 0.1, 1, and 10 kHz.

where T_0 is proportional to $\alpha^3/N(E_F)$, with α the inverse of the localization length and $N(E_F)$ the density of states at the Fermi level.[17] Indeed, the plot $\log_{10}(\sigma_{dc})$ vs $1/T^{1/4}$ leads to straight lines over a considerable temperature range (Fig. 4). In the VRH model, it is assumed that the charge carriers move away along a path determined by the optimal pair hopping rate from one localized state to another in the disorder system. Band conduction is absent because the extended states are far away from the Fermi level.[17]

C. Dielectric relaxation and ac conductivity

For all the samples investigated, dielectric loss peaks were found in the temperature range 50–200 K with frequency dispersion (see, e.g., Fig. 1), typical for a relaxational process. Due to the huge paraelectric background, the samples with $0.02 \leqslant x \leqslant 0.1$ show only weak corresponding dielectric anomalies in $\epsilon'(T)$. However, for the slow-cooling sample with $x=0.2$, the expected steplike behavior of $\epsilon'(T)$ is nicely developed (Fig. 5). The obvious dielectric peaks were observed in $\epsilon'(T)$ from 100 to 180 K in the frequency range 0.1–10 kHz; with further increasing temperature, $\epsilon'(T)$ increases quickly.

In the previous paper,[13] the dielectric relaxation process is attributed to trap-controlled ac conduction. However, the relaxing entities and the carriers of the VRH mechanism are unclear up to now. In the present work, in order to explore the nature of the dielectric relaxation and conduction mechanism, the sample with $x=0.2$ was studied in more detail. We found that the cooling rate during preparation has a strong influence on the electrical properties of the samples. As shown in Fig. 5, in contrast to the slow-cooling sample, for the quenched sample ϵ' is strongly suppressed and the dielectric peaks in the temperature range 100–180 K disappear; however, with further increasing temperature higher than 180 K, $\epsilon'(T)$ increases sharply similar to that of the slow-cooling sample. The temperature dependence of the dc conductivity for the quenched sample also follows VRH behavior, as shown in Fig. 4; only the conductivity is smaller by about half an order of magnitude. It should be pointed out that the temperature range for the sharp increase in $\epsilon'(T)$ corresponds to the temperature region in which the VRH behavior was observed.

The frequency dependence of the real part of the ac conductivity, $\sigma_{ac}(\nu)$, is shown for both samples in Fig. 6. For high temperatures, $\sigma_{ac}(\nu)$ exhibits a low-frequency plateau that can be associated with the dc conductivity. Indeed, the values for σ_{dc}, read off from the plateau in $\sigma_{ac}(\nu)$, agree well with the measured σ_{dc} as demonstrated for the slow-cooling sample in Fig. 4 (triangles). For higher frequencies a power-law behavior, $\sigma_{ac}(\nu) \sim \nu^s$ is observed. The ac conductivity then can be described by the so-called universal dielectric response,[18]

$$\sigma_{ac}(\nu) = \sigma_{dc} + A(T)\nu^s \tag{3}$$

with $s<1$. There is a vast number of theoretical approaches to deduce this behavior from the microscopic transport prop-

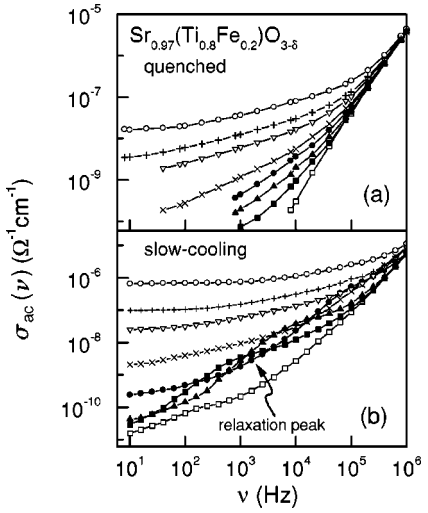

FIG. 6. Frequency dependence of the real part of the conductivity $\sigma_{ac}(\nu)$ for both samples with $x=0.2$ (slow cooled and quenched during preparation). The temperatures are (from bottom to top): 60, 100, 140, 160, 200, 240, 260, and 290 K.

erties of various classes of materials.[19] The quantum-mechanical tunneling (QMT) model, which corresponds to the VRH model for nonzero frequencies, predicts a temperature-independent frequency exponent s near 0.8.[19] Unfortunately, due to additional contributions in $\sigma_{ac}(\nu)$ (see below) an unambiguous determination of $\sigma(T)$ is difficult but at least the data do not contradict the QMT prediction.

From Fig. 6(b), it can be seen that at low temperatures, for example, 100 K, $\sigma_{ac}(\nu)$ of the slow-cooling sample exhibits an obvious shoulder in the frequency range 0.1–100 kHz, which corresponds well to the dielectric relaxation peak observed in the temperature dependence of the $\epsilon'(T)$ in Fig. 5. For the quenched sample this contribution is absent [Fig. 6(a)]. In addition, $\sigma_{ac}(\nu)$ of both samples approaches a behavior $\sigma_{ac}(\nu) \sim \nu^2$ for the highest frequencies investigated. While the used LCR meters often show some systematic errors at the highest frequencies, $\nu > 100$ kHz, we think this unusually steep increase is intrinsic, especially in light of the fact that both samples have been measured using two different devices, HP 4284 LCR meter and Solartron 1260 Impedance Gain-Phase Analyzer. Measurements at higher frequencies are necessary to explore the physical nature of the behavior.

D. Discussion

1. Conduction carrier

It is reported that $Sr_{0.97}(Ti_{1-x}Fe_x)O_{3-\delta}$ exhibits hole conduction when sintered in air (i.e., under oxidizing conditions).[11] In the present work, the conductivity of the quenched sample is lower than that of the sample made by a slow-cooling process. This phenomenon was also observed for quenched samples of high-T_c superconducting ceramic Y-Ba-Cu-O with hole conduction[20] and attributed to oxygen deficiency due to the lack of oxygen absorption during the cooling process. For both systems, the creation of holes can be described as[11]

$$O_2 + 2V_o^{\cdot\cdot} \Leftrightarrow 2O_o^{\times} + 4h^{\cdot}, \tag{4}$$

where $V_o^{\cdot\cdot}$ represents an oxygen vacancy carrying two excess positive charges, $O_o^{\times}$ means a neutral oxygen lattice site, and $h^{\cdot}$ is a hole.

2. VRH conduction

The occurrence of VRH conduction in $Sr_{0.97}(Ti_{1-x}Fe_x)O_{3-\delta}$ implies that the system is highly disordered, which might be caused by the existence of Sr vacancies, oxygen vacancies, and/or the random distribution of the Fe ions at the Ti sites.[13,21] The VRH conduction is connected with local states around the Fermi level.

In this work, the conduction carriers are holes; for Fe and Ti ions in the oxides, it is very reasonable to assume the holes could be trapped by Fe^{3+} or Ti^{3+} ions, which in general exist in this system, if the concentration of holes is high. These processes can be described by

$$Fe^{3+} + h^{\cdot} \Leftrightarrow Fe^{4+}, \tag{5}$$

$$Ti^{3+} + h^{\cdot} \Leftrightarrow Ti^{4+}. \tag{6}$$

These weakly bonded holes lead to local states around the Fermi level that give rise to the observed VRH behavior. It is possible to explain the difference of the values of the dc conductivity of the slow-cooled and quenched samples: the quenching process leads to a smaller oxygen concentration in the sample and therefore a smaller hole concentration.[11,20] Hence, σ_0 in Eq. (2) is lower than that of the slow-cooled sample and the dc conductivity value is low, but the VRH conduction mechanism remains the same.

3. Dielectric relaxation

The slow-cooling sample with $x = 0.2$ shows a dielectric relaxation mode, but the quenched sample does not. However both samples exhibit VRH conduction. It can be concluded that the dielectric relaxation process is not directly related to the VRH mechanism.

In this work, the dielectric relaxation time, determined from the loss-peak frequencies, follows a thermal activation mechanism, with an activation energy $E_{relax} = 60$ meV.[13] This value of the activation energy has a similar magnitude to that of the dielectric relaxations found in various perovskites of ABO_3 type.[22–24] These relaxation processes were attributed to localized hopping of polarons between lattice sites, which is equivalent to the reorientation of an electric dipole.[22–24] The dielectric relaxation behavior can be ascribed to a local hopping of holes between two Fe^{3+}/Fe^{4+} and/or Ti^{3+}/Ti^{4+} sites [Eq. (5) and/or (6)], which corresponds to a polaronic process. The disappearance of the dielectric relaxation in the quenched sample might be attributed to the lower hole concentration in the sample.

IV. CONCLUSION

The present work reveals some results: (i) For low concentration Fe doping, the quantum-paraelectric background remains present and the suppression of the paraelectric state is smaller than that for Bi doping and La doping. The higher stability of the quantum-paraelectric state might be due to the fact that Fe substitutes on the Ti site, in contrast to Bi and La doping. (ii) From the observed VRH conduction mechanism it can be concluded that the Fe doping generates local states in the highly disordered $SrTiO_3$ lattice; this behavior coexists with the quantum-paraelectric background. (iii) A dielectric relaxation process from 50 to 200 K is observed, which has no direct relation with the VRH process. It is very possibly related to the hopping of polarons between two Fe and/or Ti sites.

*Permanent address: Department of Physics, Department of Materials Science and Engineering, Zhejiang University, Hangzhou, 310027, P.R. China.

[1] K. A. Müller and H. Burkhard, Phys. Rev. B **19**, 3593 (1979).
[2] H. E. Weaver, J. Phys. Chem. Solids **11**, 274 (1959).
[3] T. Mitsui and W. B. Westphal, Phys. Rev. **124**, 1354 (1961).
[4] J. G. Bednorz and K. A. Müller, Phys. Rev. Lett. **52**, 2289 (1984).
[5] U. Bianchi, J. Dec, W. Kleemann, and J. G. Bednorz, Phys. Rev. B **51**, 8737 (1995).
[6] Chen Ang, Zhi Yu, P. M. Vilarinho, and J. L. Baptista, Phys. Rev.

B **57**, 7403 (1998).
[7] Chen Ang, J. F. Scott, Zhi Yu, H. Ledbetter, and J. L. Baptista, Phys. Rev. B **59**, 6661 (1999).
[8] Chen Ang, Zhi Yu, J. Hemberger, P. Lunkhemer, and A. Loidl, Phys. Rev. B **59**, 6665 (1999); Chen Ang, Zhi Yu, P. Lunkhemer, J. Hemberger, and A. Loidl, *ibid.* **59**, 6670 (1999).
[9] Zhi Yu, Chen Ang, and L. E. Cross, Appl. Phys. Lett. **74**, 3044 (1999).
[10] L. H. Brixner, Mater. Res. Bull. **3**, 299 (1968).
[11] S. Steinvik, T. Norby, and P. Kofstad, in *Electroceramics IV*, edited by R. Waser (Augustinus Buchhandlung, Aachen, 1994), Vol. II, p. 691.
[12] W. Denk, J. Munch, and J. Maier, J. Am. Ceram. Soc. **78**, 3265 (1995).
[13] Chen Ang, J. R. Jurado, Zhi Yu, M. T. Colomer, J. R. Frade, and J. L. Baptista, Phys. Rev. B **57**, 11 858 (1998).
[14] J. R. Jurado, F. M. Figueiredo, B. Gharbage, and J. R. Frade, Solid State Ionics **118**, 89 (1999).
[15] J. H. Barrett, Phys. Rev. **86**, 118 (1952).
[16] U. T. Höchli, H. E. Weibel, and L. A. Boatner, Phys. Rev. Lett. **41**, 1410 (1978).
[17] N. F. Mott and E. A. Davis, *Electronic Processes in Non-Crystalline Materials* (Clarendon Press, Oxford, 1979).
[18] A. K. Jonscher, *Dielectric Relaxation in Solids* (Chelsea Dielectrics Press, London, 1983).
[19] S. R. Elliott, Adv. Phys. **36**, 135 (1987); A. R. Long, *ibid.* **31**, 553 (1982).
[20] *Physical Properties of High Temperature Superconductors I, II*, edited by D. M. Ginsberg (World Scientific, Singapore, 1989).
[21] D. H. Liu, X. Yao, and L. E. Cross, J. Appl. Phys. **71**, 5115 (1992).
[22] O. Bidault, M. Maglione, M. Actis, M. Kchikech, and B. Salce, Phys. Rev. B **52**, 4191 (1995).
[23] E. Iguchi, N. Kubota, T. Nakamori, N. Yamamoto, and K. J. Lee, Phys. Rev. B **43**, 8646 (1991).
[24] M. Maglione, Ferroelectrics **176**, 1 (1996).